View metadata, citation and similar papers at core.ac.uk

brought to you by CORE

provided by Elsevier - Publisher Connector

© 2010 International Society of Nephrology

see commentary on page 333

Pivotal role of CD4$^+$ T cells in renal fibrosis following ureteric obstruction

Thomas T. Tapmeier[1], Amy Fearn[2], Kathryn Brown[1], Paramit Chowdhury[1], Steven H. Sacks[1], Neil S. Sheerin[2] and Wilson Wong[1]

[1]*MRC Centre for Transplantation, King's College London School of Medicine at Guy's, King's and St Thomas' Hospitals, London, UK and* [2]*Institute of Cellular Medicine, Newcastle University, Newcastle upon Tyne, UK*

Tubulointerstitial fibrosis is a common consequence of a diverse range of kidney diseases that lead to end-stage renal failure. The degree of fibrosis is related to leukocyte infiltration. Here, we determined the role of different T cell populations on renal fibrosis in the well-characterized mouse model of unilateral ureteric obstruction. Depletion of CD4$^+$ T cells in wild-type mice with a monoclonal antibody significantly reduced the amount of interstitial expansion and collagen deposition after 2 weeks of obstruction. Reconstitution of lymphopenic *RAG* knockout mice with purified CD4$^+$ but not CD8$^+$ T cells, prior to ureteric obstruction, resulted in a significant increase in interstitial expansion and collagen deposition. Wild-type mice had significantly greater interstitial expansion and collagen deposition compared with lymphopenic *RAG*$^{-/-}$ mice, following ureteric obstruction; however, macrophage infiltration was equivalent in all groups. Thus, our results suggest that renal injury with subsequent fibrosis is likely to be a multifactorial process, with different arms of the immune system involved at different stages. In this ureteric obstruction model, we found a critical role for CD4$^+$ T cells in kidney fibrosis. These cells could be a potential target of therapeutic intervention to prevent excessive fibrosis and loss of function due to renal injury.

Kidney International (2010) **78,** 351–362; doi:10.1038/ki.2010.177; published online 16 June 2010

KEYWORDS: CD4$^+$ T cells; fibrosis; ureteric obstruction

Correspondence: *Wilson Wong, MRC Centre for Transplantation, 5th Floor, Tower Wing, Guy's Hospital, London SE1 9RT, UK.*
E-mail: wilson.wong@kcl.ac.uk

Received 9 October 2008; revised 29 March 2010; accepted 21 April 2010; published online 16 June 2010

The common end point of virtually all types of progressive renal disease is tubulointerstitial fibrosis.[1] Although fibrosis is a normal physiological process—in response to persisting tissue injury—if left unchecked, it can lead to abnormal tissue remodeling and permanent scarring. Severity of interstitial fibrosis is an accurate predictor of kidney survival.[2] Chronic kidney disease also shows widespread lymphocyte infiltration into the kidney. T cells have been detected in kidneys of patients with chronic kidney disease,[3] as well as in models of renal fibrosis such as unilateral ureteric obstruction (UUO).[4–7] Furthermore, in CCR1$^{-/-}$ animals, or when CCR1 function is blocked, there is reduced lymphocyte infiltration and fibrosis in the kidney after UUO.[4,6]

The role of different T-cell populations in the development of glomerular injury has been studied with CD8$^+$ T effector cells implicated in adriamycin-induced nephritis[8] and a CD4$^+$ T_H1 response in nephrotoxic nephritis models.[9] However, no *in vivo* study has directly addressed the role of different T-cell populations in renal fibrosis, despite the importance of fibrosis in renal progression and chronic kidney disease.

In this study, we depleted wild-type (WT) C57BL/6 mice of CD4$^+$ T cells using a monoclonal antibody, and subsequently reconstituted syngeneic recombination activation gene-1 *(RAG)* knockout mice[10] with either CD4$^+$ T cells or CD8$^+$ T cells from WT donors to dissect the role of T cells in UUO-induced renal fibrosis.

RESULTS

Depletion of CD4$^+$ T cells results in reduced interstitial expansion and collagen deposition after UUO

To investigate the role of CD4$^+$ T cells in renal injury and fibrosis after UUO, C57BL/6 mice were administered 50 μg of depleting anti-CD4 antibody intravenously on two consecutive days, and were obstructed on the second day. In peripheral blood, only 0.3% ± 0.2% of all cells in the mononuclear gate were CD4$^+$ at 2 days after depletion compared with 20.9% ± 4.5% in naive mice ($n = 7$; Figure 1a–c), whereas CD8$^+$ T cells remained at 16.0% ± 4.5% ($n = 7$). By day 14, CD4$^+$ T cells reemerged, with 6.4% ± 1.8% of cells within the mononuclear gate staining positive for CD4 ($n = 7$; Figure 1d).

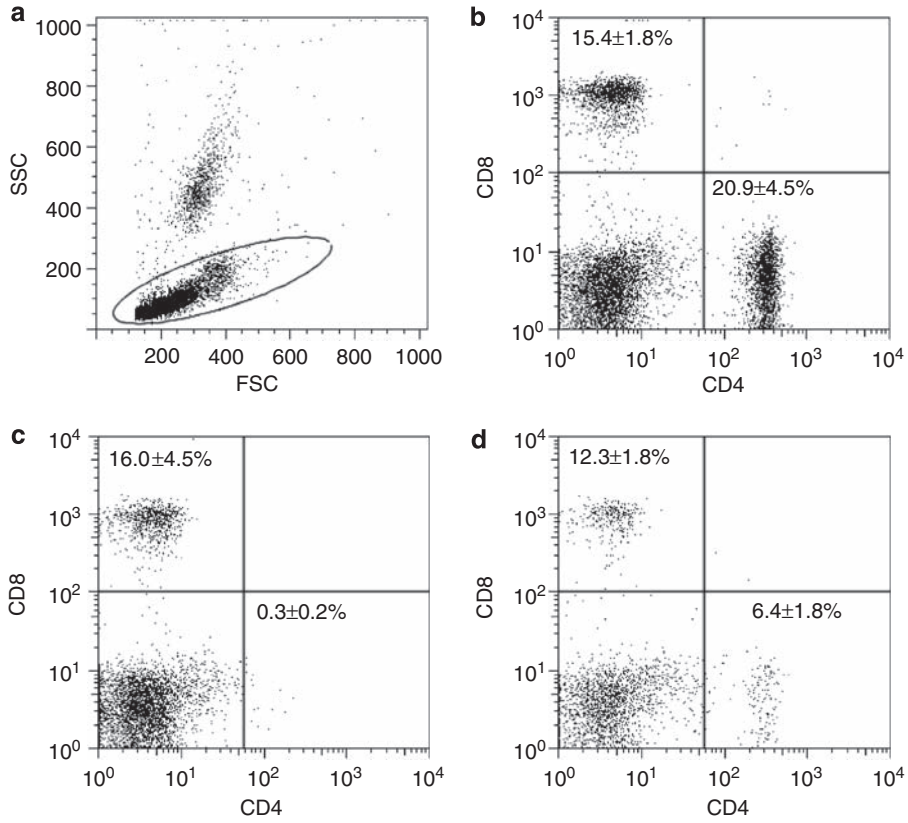

Figure 1 | Depletion of CD4+ T cells from C57BL/6 mice. Mice were injected with 50 μg of depleting anti-CD4 antibody (intravenously) on two consecutive days. Blood samples were taken on day 2 and day 14 after the second dose of antibody, and analyzed for the presence of $CD4^+$ and $CD8^+$ T cells by flow cytometry. Mean percentages ± s.d. are given in each plot. (**a**) A lymphoid gate was used to analyze T cells; side scatter (SSC); forward scatter (FSC). (**b**) Wild-type control mice ($n=7$) showed both $CD4^+$ and $CD8^+$ T cells in their blood. (**c**) At day 2 after depletion, $CD4^+$ T cells are absent from the blood ($n=7$). $CD8^+$ T cells are unaffected. (**d**) By day 14 after depletion, $CD4^+$ T cells start to reemerge in the circulation ($n=7$).

$CD4^+$ T cell-depleted mice underwent UUO surgery and the obstructed kidneys were harvested 14 days later for histological analysis. Interstitial expansion and collagen deposition were quantified on periodic acid Schiff's reagent- and Martius scarlet blue trichrome-stained sections, respectively (Figure 2a, b, g and h). Interstitial expansion in obstructed kidneys from CD4-depleted mice was significantly lower, with 36.6% ± 2.0% ($n=7$) of the cortex occupied by the interstitium compared with saline-treated controls showing 49.4% ± 3.1% ($n=5$; $P=0.0025$; Figure 3a). In control mice, 41.1% ± 1.1% ($n=6$) of the cortex stained positive for collagen; depleted mice showed significantly less staining, 23.74% ± 2.1% ($n=7$; $P=0.0012$; Figure 3b). Tubular dilatation, as measured by the ratio of tubular diameter to epithelial cell height, was similar in both groups (7.4 ± 1.0 and 6.0 ± 0.8, naive and treated group, respectively, Figure 3c). Immunohistochemical analysis of the affected kidneys showed $CD4^+$ cells present in both groups at the time of sample harvest (despite the earlier depletion in peripheral blood, Figure 2m and n) (21.8 ± 1.5 $CD4^+$ cells/high power field (hpf) ($n=5$), 15.23 ± 1.7 $CD4^+$ cells/hpf ($n=7$); $P=0.0189$; Figure 3d, naive and treated group, respectively). The analysis of $CD8^+$ cells in the affected kidneys (Figure 2s and t) showed 9.4 ± 0.6 $CD8^+$ cells/hpf in WT mice ($n=5$) and 20.8 ± 2.7 $CD8^+$ cells/hpf in depleted mice ($n=7$; $P=0.0028$; Figure 3e). The infiltration of macrophages as documented by the area staining positive for F4/80 (Figure 2y and z) was similar in both groups (Figure 3f; 37.2% ± 0.9% $F4/80^+$ ($n=6$) and 36.8% ± 1.3% $F4/80^+$ ($n=7$), naive and treated group, respectively). The depletion of $CD4^+$ cells did not seem to reduce the amount of α-SMA^+ (alpha smooth muscle action) cells in affected kidneys (Supplementary Figure S1); however, as the depletion of renal $CD4^+$ cells was incomplete, the relation of myofibroblasts and lymphocytes could not be elucidated sufficiently by this approach.

The reemergence of $CD4^+$ T cells and increased infiltration of $CD8^+$ T cells in the treated group also make it difficult to ascribe the decrease in interstitial expansion and collagen deposition observed in the depleted mice to either $CD4^+$ or $CD8^+$ T-cell populations. To systematically dissect the roles of these T-cell populations in the UUO model, we used lymphopenic $RAG^{-/-}$ mice and extended the analysis to additional parameters of renal fibrosis.

Lymphopenic $RAG^{-/-}$ mice develop less fibrotic injury after UUO

$RAG^{-/-}$ mice underwent UUO for 14 days before tissue was harvested for histological analysis. Interstitial expansion was

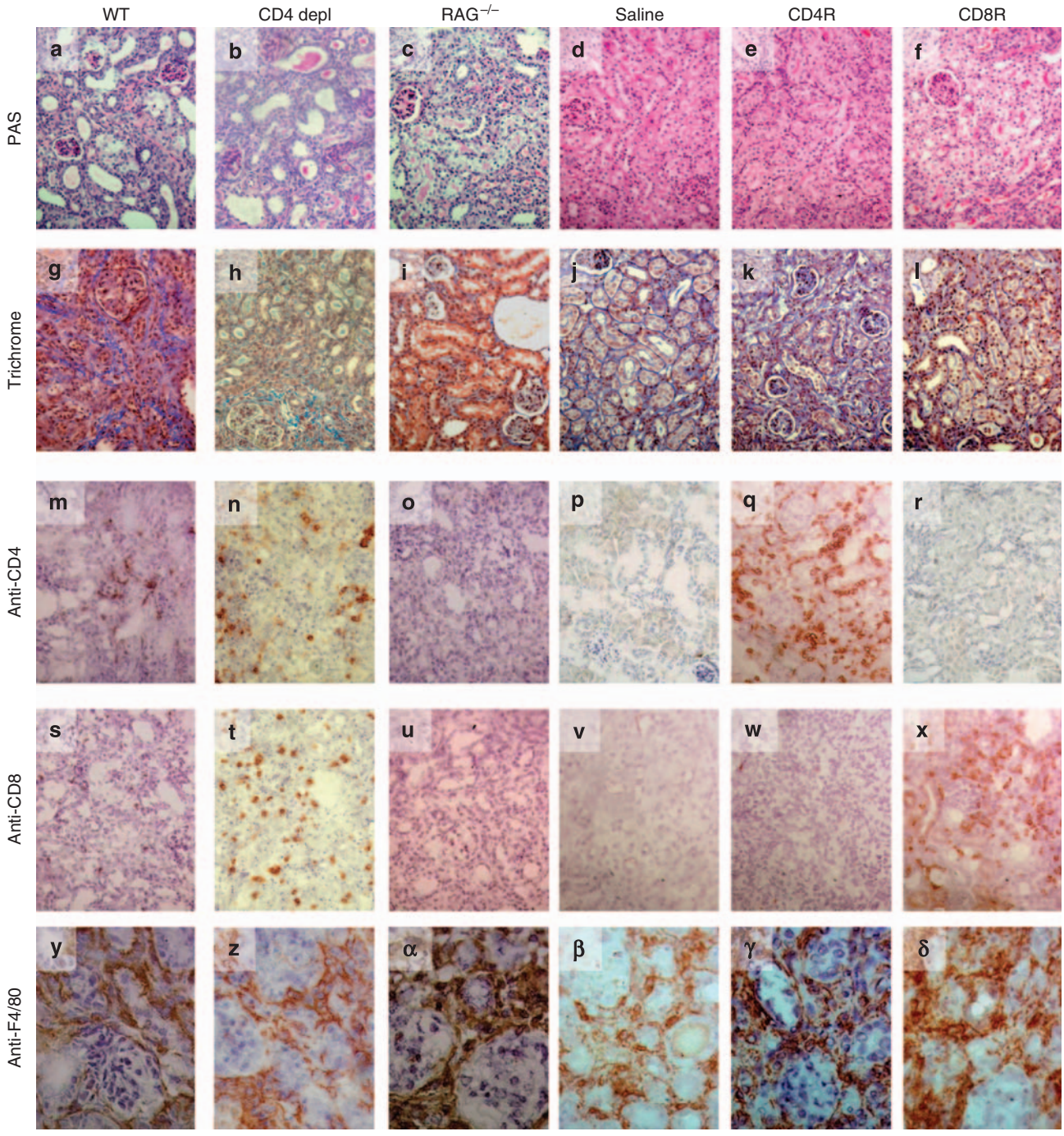

Figure 2 | Histological and immunohistochemical analysis of fibrosis and leukocyte infiltration after unilateral ureteric obstruction. Representative images of renal cortex sections of affected kidneys of mice after 14 days of unilateral ureteric obstruction are shown. Experimental groups are wild type (WT), CD4-depleted mice (CD4 depl), *RAG*$^{-/-}$, *RAG*$^{-/-}$ mice reconstituted with saline (saline), CD4$^+$ T cells (CD4R), and CD8$^+$ T cells (CD8R). (**a**–**f**) Periodic acid/Schiff's reagent (PAS) stains demonstrating interstitial expansion in affected kidneys. This was more severe in WT (**a**) compared with CD4-depleted (**b**) and *RAG*$^{-/-}$ mice (**c**), and more severe in CD4R mice (**e**) than in saline (**d**) or CD8R mice (**f**). (**g**–**l**) Martius scarlet blue (MSB) trichrome stains showing interstitial collagen deposition (blue) in affected kidneys. The highest degree of collagen deposition was observed in WT (**g**) and CD4R (**k**) mice, less was seen in CD4-depleted (**h**), *RAG*$^{-/-}$ (**i**), saline (**j**), and CD8R mice (**l**). (**m**–**r**) Sections stained with anti-CD4 antibody show infiltrating CD4$^+$ cells in WT (**m**), CD4-depleted (**n**), and CD4R mice (**q**), whereas CD4$^+$ cells were observed only occasionally in *RAG*$^{-/-}$ (**o**), saline (**p**), and CD8R mice (**r**). (**s**–**x**) Anti-CD8 staining showing infiltration of CD8$^+$ cells in WT (**s**), CD4-depleted (**t**) and CD8R mice (**x**), whereas no CD8$^+$ cells were seen in *RAG*$^{-/-}$ (**u**), saline (**v**), and CD4R mice (**w**). (**y**–**δ**) Macrophages were documented as F4/80$^+$ cells. A similar level of macrophage infiltration was seen in all groups. Magnification $\times$400 for PAS, MSB trichrome, anti-CD4, and anti-CD8 stains, $\times$1000 for F4/80 stain.

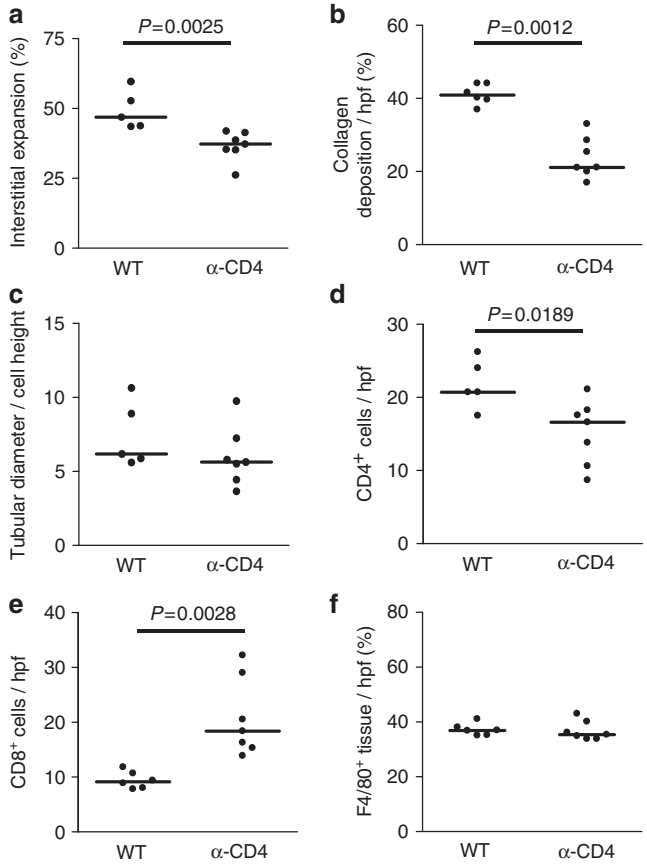

Figure 3 | Analysis of interstitial collagen deposition and leukocyte infiltration in affected kidneys of WT and CD4$^+$ T cell-depleted mice after 14 days of unilateral ureteric obstruction (UUO). Mice were depleted on two consecutive days by injection of 50 μg anti-CD4 antibody (intravenously). UUO surgery was performed on the second day, and samples were harvested after 14 days. Interstitial expansion, collagen deposition, and macrophage infiltration in affected kidneys of wild-type (WT) and *RAG*$^{-/-}$ mice were quantified using a scoring grid. Infiltration of CD4$^+$ and CD8$^+$ cells is given as cell counts per high power field (hpf). Graphs show data and medians. (**a**) Mice depleted of CD4$^+$ T cells ($n=7$) showed reduced interstitial expansion compared with WT mice ($n=5$) as quantified on PAS stains. (**b**) CD4-depleted mice showed less collagen deposition in the interstitium than WT mice, as quantified on Martius scarlet blue trichrome stains. (**c**) Tubular dilatation was similar between WT and CD4-depleted mice. (**d**) The number of CD4$^+$ T cells infiltrating the affected kidneys of CD4-depleted mice is reduced compared with WT mice. (**e**) The number of infiltrating CD8$^+$ T cells is increased in CD4$^+$ T cell-depleted mice compared with WT mice. (**f**) The infiltration of macrophages as quantified on F4/80$^+$ tissue is similar in depleted and WT mice.

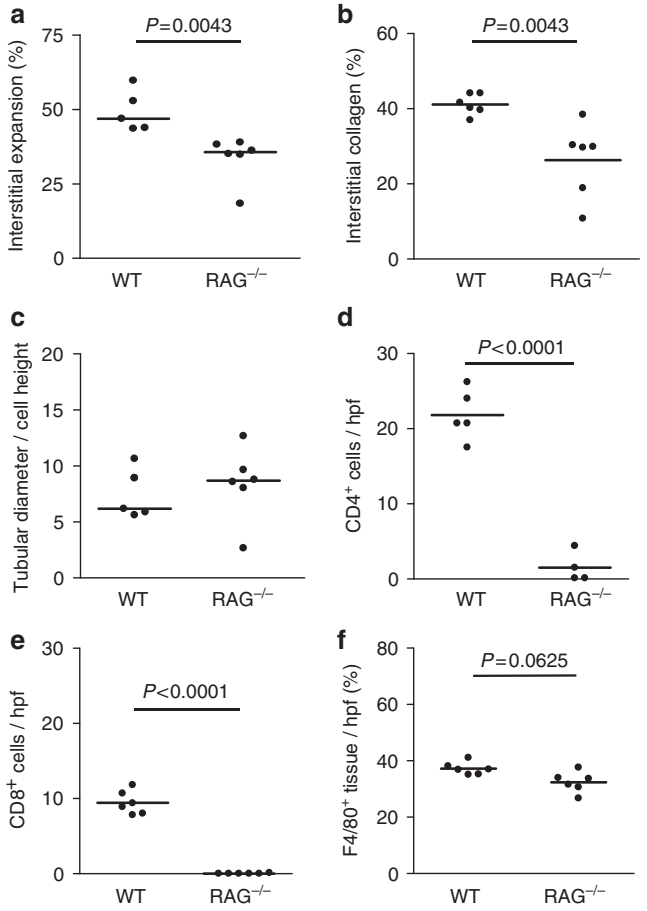

Figure 4 | Lymphocyte deficiency protects *RAG*$^{-/-}$ mice from fibrosis induced by 14 days of unilateral ureteric obstruction. Interstitial expansion, collagen deposition, and macrophage infiltration in affected kidneys of wild-type (WT) and *RAG*$^{-/-}$ mice were quantified using a scoring grid. Infiltration of CD4$^+$ and CD8$^+$ cells is given as cell counts per high power field. The WT data from Figure 3 are shown here again for easier comparison. Graphs show data and medians. (**a**) Interstitial expansion was significantly lower in *RAG*$^{-/-}$ mice ($n=6$) compared with WT mice ($n=7$). (**b**) Interstitial collagen deposition in *RAG*$^{-/-}$ mice was reduced compared with WT mice. (**c**) Tubular dilatation was not different between WT and *RAG*$^{-/-}$ mice. (**d**) Infiltration of CD4$^+$ cells was observed in WT but not in *RAG*$^{-/-}$ mice. (**e**) Infiltration of CD8$^+$ cells was observed in WT mice but not in *RAG*$^{-/-}$ mice. (**f**) The infiltration of macrophages was similar in *RAG*$^{-/-}$ and WT mice.

found to be significantly lower in the obstructed kidneys of *RAG*$^{-/-}$ mice ($n=6$) compared with WT controls ($n=5$), (33.6% ± 3.1% versus 49.4 ± 3.1%, $P=0.0043$; Figures 2a, c and 4a). Unaffected contralateral kidneys showed little injury as expected (Supplementary Figure S1).

When collagen deposition was assessed on Martius scarlet blue trichrome-stained sections, *RAG*$^{-/-}$ mice showed significantly less collagen deposition after UUO than did WT controls, 26.3% ± 4.0% and 41.1% ± 1.1%, respectively ($P=0.0043$, $n=6$; Figures 3g, i and 4b). Tubular dilatation was similar in both groups, 7.4 ± 1.0 and 8.4 ± 1.3 in *RAG*$^{-/-}$ and WT, respectively, indicating equally obstructed kidneys (Figure 4c).

Macrophage and T-cell infiltration of obstructed kidneys

Immunohistochemical analysis showed heavy infiltration by both CD4$^+$ and CD8$^+$ T cells in affected WT kidneys: 21.8 ± 1.5 ($n=5$) CD4$^+$ cells/hpf (Figures 2m and 4d) and 9.4 ± 0.6 ($n=6$) CD8$^+$ cells/hpf (Figures 2s and 4e). Affected *RAG*$^{-/-}$ kidneys showed a low level of CD4$^+$ staining with 1.5 ± 1.0 CD4$^+$ cells/hpf ($n=6$; $P<0.0001$; WT versus

RAG$^{-/-}$; Figures 2o and 4d). This may be due to other cells expressing CD4, for example, dendritic cells, as no T lymphocytes were found in peripheral blood samples of these mice. No CD8$^+$ cells were seen ($n=6$; $P<0.0001$; WT versus *RAG*$^{-/-}$; Figures 2u and 4e). As observed before, macrophage infiltration was unaffected by the absence of lymphocytes, as *RAG*$^{-/-}$ animals had a similar level of macrophage infiltration compared with WT, 32.4% ± 3.7% positive staining per hpf and 37.2% ± 2.2% per hpf, respectively ($n=6$ in both groups; $P=0.0625$; Figures 2y, α and 4f). Unaffected contralateral kidneys showed little cellular infiltration as expected (Supplementary Figure S1).

Reconstitution of *RAG*$^{-/-}$ mice with CD4$^+$ or CD8$^+$ T cells

To investigate the role of different subsets of T cells, *RAG*$^{-/-}$ mice were reconstituted with purified CD4$^+$ or CD8$^+$ T cells 2 weeks before UUO. We have previously shown that the absolute numbers of T cells was one-fifth to one-third of that seen in WT mice 14 days after reconstitution.[11] Reconstitution was confirmed in peripheral blood (Figure 5). In CD4$^+$ T cell-reconstituted mice, 8.05% ± 3.02% of peripheral blood leukocytes stained positive for CD4 ($n=5$; Figure 5b). In CD8$^+$ T cell-reconstituted mice, 16.59% ± 3.88% of peripheral blood leukocytes stained positive for CD8 ($n=5$; Figure 5c). In naive WT mice, the respective frequencies were 13.82% ± 2.0% CD4$^+$ and 12.6% ± 1.0% CD8$^+$ lymphocytes ($n=10$; Figure 5d). It is important to note that animals reconstituted with CD4$^+$ T cells did not show CD8$^+$ T cells, animals reconstituted with CD8$^+$ T cells did not show CD4$^+$ T cells, and saline-injected mice showed neither (Figure 5a).

Obstructed kidneys of RAG$^{-/-}$ mice show infiltrates of the respective T-cell population after reconstitution with CD4$^+$ or CD8$^+$ T cells

Although both CD4$^+$ and CD8$^+$ T cells were found in WT kidneys after UUO, it needed to be established whether the T cells used to reconstitute *RAG*$^{-/-}$ mice would behave in a similar manner. Immunohistochemical analysis of obstructed kidneys from CD4$^+$- and CD8$^+$-reconstituted animals showed high numbers of the appropriate T-cell subset infiltrating the kidney. There was a mean of 100 ± 8.8 CD4$^+$ T cells/hpf in kidneys from CD4$^+$-reconstituted mice ($n=9$, Figures 2q and 6d), whereas CD8$^+$-reconstituted

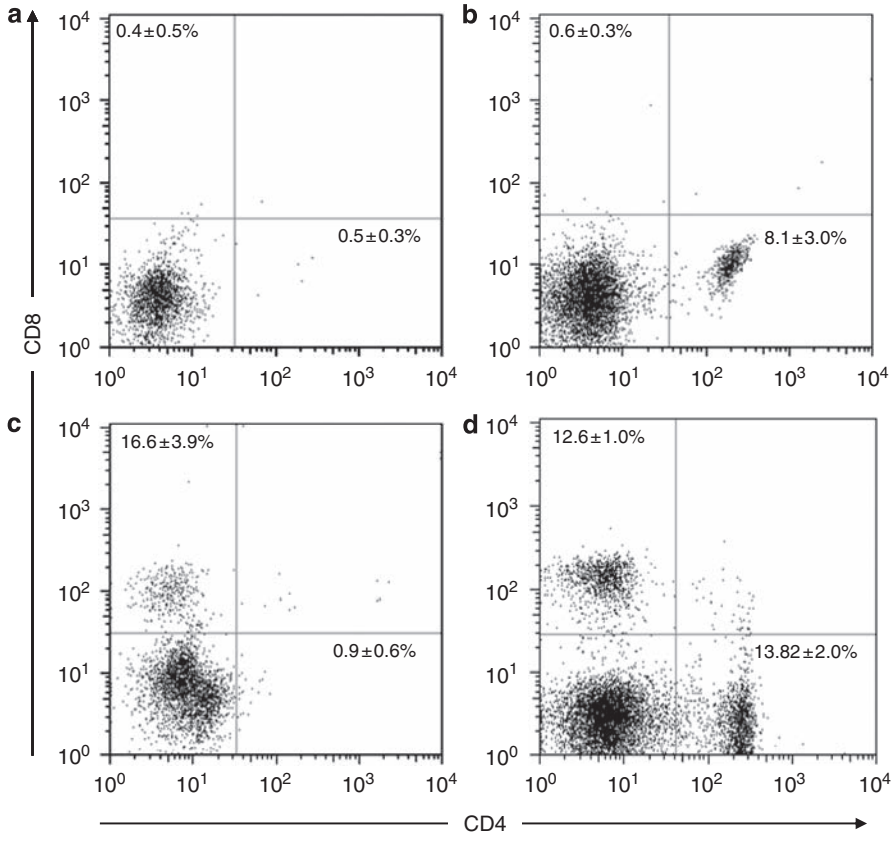

Figure 5 | Selective reconstitution of *RAG*$^{-/-}$ mice with either CD4$^+$ or CD8$^+$ T cells. At 13 days after reconstitution and 1 day before unilateral ureteric obstruction surgery, peripheral blood samples were analyzed for the presence of CD4$^+$ and CD8$^+$ cells by flow cytometry. (**a**) *RAG*$^{-/-}$ mice reconstituted with saline ($n=5$), (**b**) *RAG*$^{-/-}$ mice reconstituted with CD4$^+$ T cells ($n=5$), (**c**) *RAG*$^{-/-}$ mice reconstituted with CD8$^+$ T cells ($n=5$), (**d**) wild-type (WT) mice ($n=10$). Mean percentages ± s.d. are given in each plot. No CD4$^+$ or CD8$^+$ cells were found in the blood of saline-reconstituted *RAG*$^{-/-}$ mice, and T cell-reconstituted *RAG*$^{-/-}$ mice showed only the appropriate population in their blood, whereas WT mice showed both CD4$^+$ and CD8$^+$ cells.

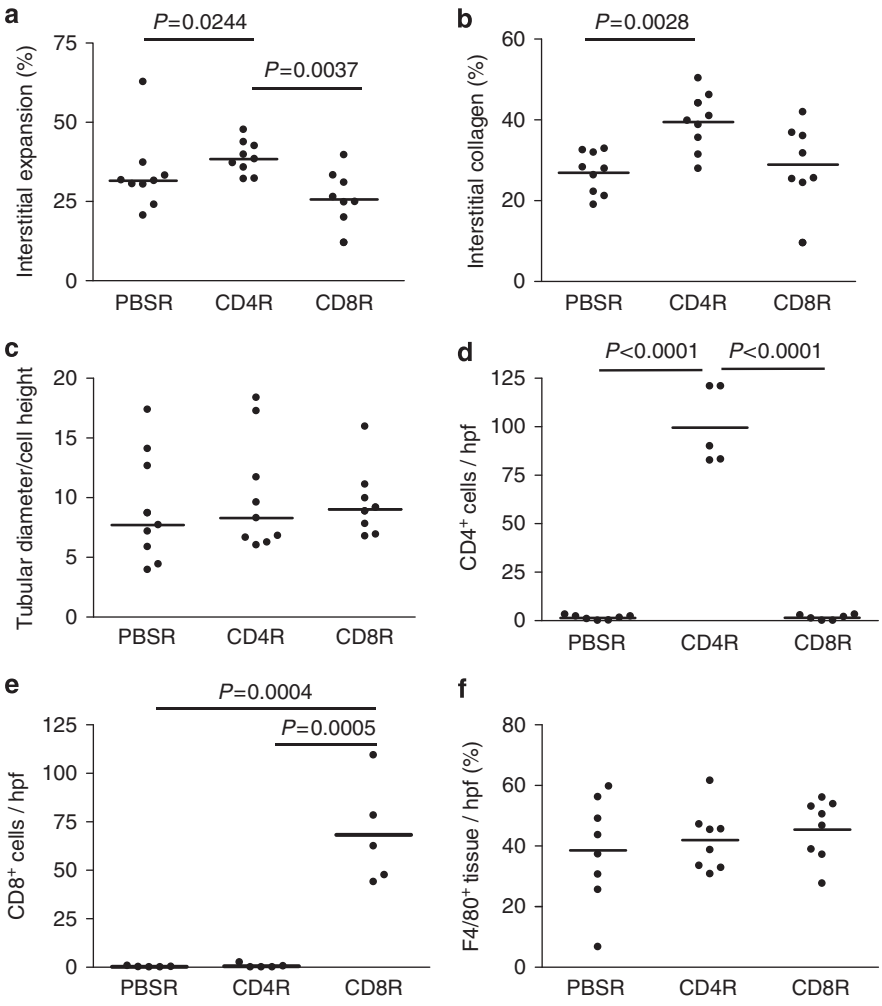

Figure 6 | Reconstitution of *RAG*$^{-/-}$ mice with CD4$^+$ T cells restores fibrosis. After 14 days of unilateral ureteric obstruction, the degree of tubulointerstitial fibrosis and leukocyte infiltration was compared between *RAG*$^{-/-}$ mice reconstituted with CD4$^+$ T cells (CD4R) or CD8$^+$ T cells (CD8R) and phosphate-buffered saline-reconstituted controls (PBSR). Interstitial expansion, collagen deposition, and macrophage infiltration were quantified by scoring grid. Infiltration of CD4$^+$ and CD8$^+$ cells is given as cells per high power field. Data are expressed as percentage of tissue showing macrophage infiltration, interstitial expansion, and collagen deposition, respectively. Tubular dilatation was calculated as the ratio of inner tubular area to epithelial cell height. Graphs show data and median. (**a**) Interstitial expansion was highest in CD4R mice, whereas saline and CD8R mice were similar ($n = 9$ in each group). (**b**) CD4R mice showed significantly more collagen deposition than saline-reconstituted *RAG*$^{-/-}$ mice, whereas CD8R mice were not different from saline mice. (**c**) Tubular dilatation was similar in all reconstituted groups. (**d**) After reconstitution, CD4R mice ($n = 5$) showed high numbers of infiltrating CD4$^+$ cells compared with saline-reconstituted mice ($n = 7$) and CD8R ($n = 5$) mice. (**e**) Reconstituted CD8R mice showed high numbers of infiltrating CD8$^+$ cells, which were absent in saline reconstituted mice and CD4R mice. (**f**) Macrophage infiltration was similar in saline-reconstituted, CD4R, and CD8R mice.

mice showed 1.5 ± 1.4 CD4$^+$ T cells/hpf ($P < 0.0001$, $n = 9$, Figures 2r and 6d) and saline-reconstituted animals showed 1.7 ± 1.1 CD4$^+$ cells/hpf ($P < 0.01$, $n = 9$, Figures 2p and 6d). Animals reconstituted with CD8$^+$ T cells showed a mean of 68 ± 11.9 CD8$^+$ cells/hpf in obstructed kidneys (Figures 2x and 6e), whereas CD4$^+$-reconstituted mice showed 0.6 ± 1.1 CD8$^+$ cells/hpf ($P < 0.0005$, Figures 2w and 6e) and saline-reconstituted mice showed 0.3 ± 0.3 CD8$^+$ cells/hpf ($P < 0.001$, Figures 2v and 6e). The infiltration of macrophages as assessed by scoring F4/80-positive tissue was similar in all groups, with a mean of $38.6\% \pm 17.5\%$ of F4/80-positive stained tissue area per hpf in saline-reconstituted mice, a mean of $41.9\% \pm 10.2\%$ of F4/80-positive tissue in CD4$^+$-reconstituted animals, and a mean of $45.5\% \pm 10.0\%$ of F4/80-positive tissue in CD8$^+$-reconstituted mice (Figures 2β–δ and 6f).

CD4$^+$ but not CD8$^+$ T cells restore the severity of UUO-induced renal fibrosis in *RAG*$^{-/-}$ mice

To investigate the effect of infiltrating CD4$^+$ and CD8$^+$ T cells on renal fibrosis, we compared the interstitial area in obstructed kidneys from *RAG*$^{-/-}$ mice reconstituted with CD4$^+$ or CD8$^+$ T cells with the amount observed in saline-injected *RAG*$^{-/-}$ mice (Figure 6a). After 14 days of UUO, the interstitial area seen in CD4$^+$-reconstituted animals was $38.8\% \pm 1.7\%$ ($n = 9$) and significantly more than that seen

in saline-reconstituted animals, in which it was 33.6% ± 4.0% ($n = 9$; $P = 0.0244$ CD4R versus saline). However, the interstitial area seen in CD8+-reconstituted mice was similar to that of saline-reconstituted mice, with a score of 26.5% ± 3.0% ($n = 8$; $P = 0.3213$ CD8R versus saline).

The percentage of the total cortical area of obstructed kidneys staining positive for collagen in saline-reconstituted $RAG^{-/-}$ mice was 26.9% ± 1.7%. In CD4+-reconstituted animals, it was 39.5% ± 2.4% ($n = 9$), significantly higher than that in saline-reconstituted mice ($P = 0.0028$ CD4R versus saline; Figure 6b) and equivalent to that seen before in WT mice (Figure 4b). The percentage for CD8+-reconstituted mice was 28.9% ± 3.6% ($n = 9$), which was similar to that seen in phosphate-buffered saline-reconstituted mice (Figure 6b). To assess the severity of renal obstruction induced by UUO, the degree of tubular dilatation was determined in all reconstituted groups and was found to be similar, with saline-reconstituted mice showing a ratio of tubular diameter to epithelial cell height of 9.1 ± 1.5, CD4+ T cell-reconstituted animals showing a ratio of 10.1 ± 1.6, and animals reconstituted with CD8+ T cells a ratio of 9.6 ± 1.1 (Figure 6c).

Taken together, reconstitution with CD4+ T cells increases the severity of renal fibrosis in $RAG^{-/-}$ mice to the degree seen in WT mice, whereas reconstitution with CD8+ T cells does not.

CD4+ T cells increase collagen I gene expression

To further characterize the mechanism by which CD4+ T cells contribute to fibrotic disease in the UUO model, we analyzed the protein expression of α-SMA as a marker for myofibroblast infiltration by immunohistochemistry, as well as the mRNA expression of α-SMA, transforming growth factor (TGF)-β1, and collagen I in reconstituted animals and in WT mice. In all cases, we compared the expression of the respective fibrosis marker in the obstructed kidney with the expression in the contralateral kidney. Immunohistochemical analysis showed the presence of α-SMA+ cells in affected kidneys in all groups. SMA+ cells were only present in blood vessel walls in contralateral unobstructed kidneys (Figure 7a–h). The quantification of α-SMA staining showed significantly greater α-SMA staining in the affected kidneys compared with the contralateral kidneys (Figure 7i). When comparing the affected kidneys only, α-SMA staining in the WT group was significantly greater than that in the other groups. Reconstitution of mice with CD4+ T cells did not restore the level of α-SMA staining to that seen in WT mice. Surprisingly, $RAG^{-/-}$ mice reconstituted with CD4+ T cells showed significantly less α-SMA+ tissue than the other reconstituted groups.

The analysis of α-SMA mRNA expression (Figure 8a) showed a higher expression of α-SMA mRNA in the affected kidneys of WT and CD4+ T cell-reconstituted mice compared with contralateral kidneys. However, in saline- and CD8+ T cell-reconstituted mice, no significant difference was seen between affected and contralateral kidneys.

In all groups, except CD8+ T cell-reconstituted mice, the expression of TGF-β1 mRNA was significantly higher in affected kidneys than in contralaterals (Figure 8b). However, the expression of TGF-β1 mRNA in affected kidneys of the WT and reconstituted groups was overall not significantly different between groups ($P = 0.3715$; Kruskal–Wallis test of affected groups).

The analysis of collagen I mRNA expression showed significantly higher levels of mRNA in the affected kidneys of all groups compared with contralateral kidneys (Figure 8c), again with the exception of CD8+ T cell-reconstituted animals, which did not show a significant difference between affected and contralateral kidneys. When comparing the amount of collagen I mRNA between affected groups ($P = 0.0004$; Kruskal–Wallis test), saline-reconstituted mice showed a significantly lower expression of collagen I compared with WT mice ($P = 0.0205$, WT versus saline). Animals reconstituted with CD4+ T cells showed significantly higher levels of collagen I expression than saline-reconstituted $RAG^{-/-}$ mice ($P < 0.0001$, CD4R versus phosphate buffered saline reconstitute (PBSR)) and were not different from WT mice. However, reconstitution with CD8+ T cells failed to restore collagen I expression in affected kidneys to the WT level and resulted in collagen I expression that was significantly lower than that seen in CD4+ T cell-reconstituted animals ($P = 0.0002$, CD8R versus CD4R).

Thus, after reconstitution with CD4+ T cells, expression of α-SMA, TGF-β1, and collagen I is significantly upregulated in affected kidneys compared with contralaterals, whereas after reconstitution with CD8+ T cells, it is not. This is consistent with the histological findings of greater injury after CD4+ T-cell reconstitution than after reconstitution with CD8+ T cells, and with a role for CD4+ T cells in renal fibrosis after UUO.

DISCUSSION

Renal fibrosis is a common end point of many progressive kidney diseases. Understanding its pathophysiology may lead to effective therapies to prevent the progression of kidney disease and renal failure.

We adopted a CD4+ T-cell depletion protocol shown to be effective in inducing transplant tolerance to cardiac allografts[12] to determine whether this would reduce the severity of renal fibrosis after UUO. Although initial deletion of peripheral CD4+ T cells was nearly complete, there was some recovery toward the end of the 14-day period. More important, CD4+ T-cell infiltration was still seen in the affected kidneys. Nevertheless, we observed a significantly lower level of fibrosis after anti-CD4 monoclonal antibody treatment. However, we also saw a corresponding rise in the amount of CD8+ T cells in affected kidneys. The reason for this is not immediately apparent.

To further dissect the role of T cells in fibrosis following UUO, we used $RAG^{-/-}$ mice to avoid the complicated consequences that we observed after CD4+ T-cell depletion. We found significantly less interstitial expansion and collagen

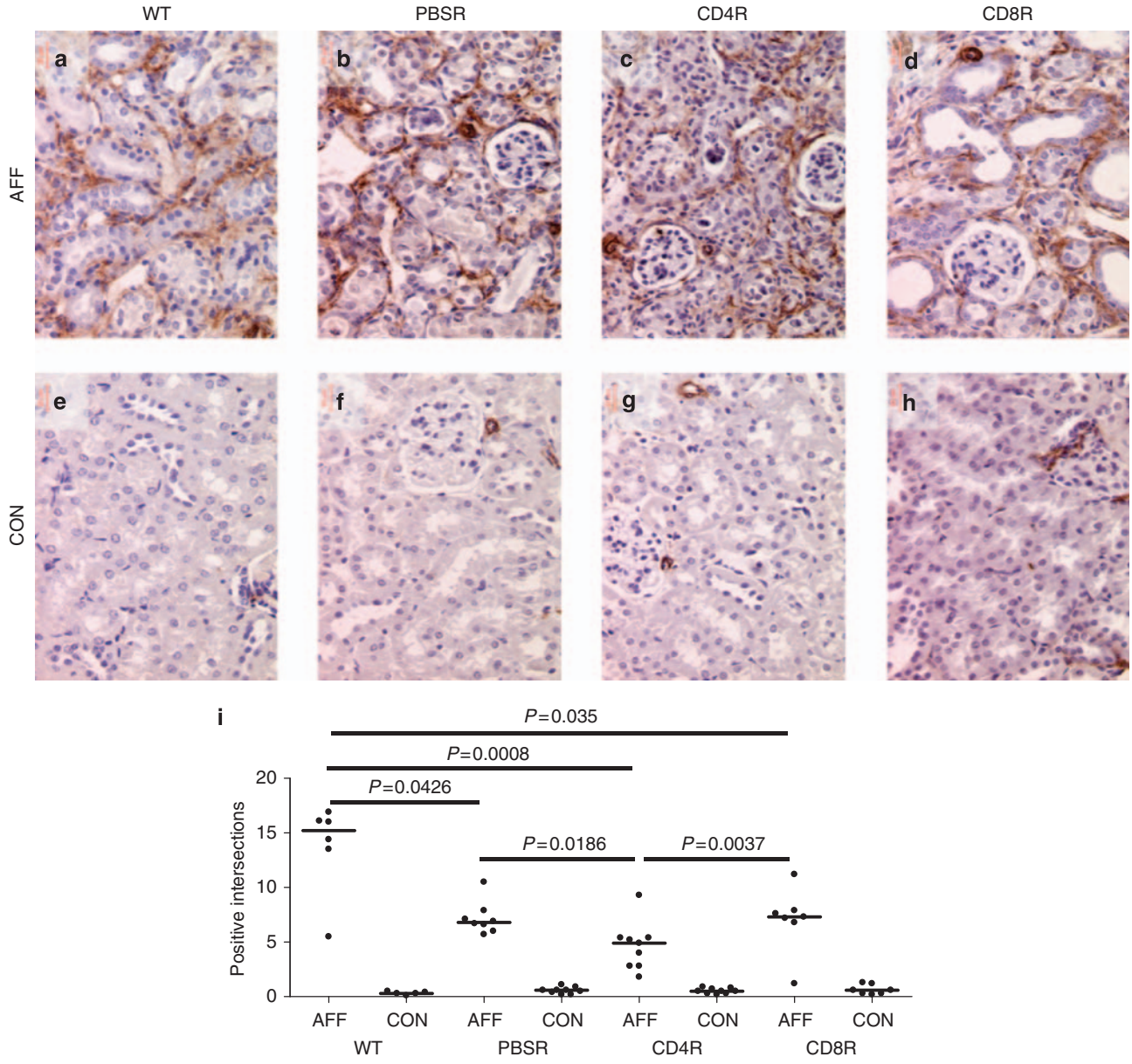

Figure 7 | Expression of α-SMA in affected kidneys of WT and reconstituted *RAG*$^{-/-}$ mice. (**a**–**h**) Representative renal cortical sections of affected (AFF) and contralateral (CON) kidneys from wild-type (WT) and reconstituted *RAG*$^{-/-}$ mice stained with anti-α-SMA antibody. In all groups, interstitial infiltration of α-SMA^{+} cells was documented in affected kidneys but not in contralateral kidneys. (**i**) Quantification of α-SMA^{+} tissue by scoring grid. All groups of reconstituted *RAG*$^{-/-}$ mice showed significantly less α-SMA^{+} tissue than WT mice. Within reconstituted groups, *RAG*$^{-/-}$ mice reconstituted with CD4^{+} T cells showed significantly less α-SMA^{+} tissue than the other reconstituted groups.

deposition in *RAG*$^{-/-}$ mice compared with WT mice. As macrophages are present in similar numbers in both groups, whereas T and B cells are absent in *RAG*$^{-/-}$ mice, these lymphocytes are likely to have a significant role in the development of fibrosis in this model. The presence of CD4^{+} and CD8^{+} T cells in obstructed kidneys from WT mice after UUO supports this hypothesis. To investigate this further, *RAG*$^{-/-}$ mice were reconstituted with either CD4^{+} or CD8^{+} T cells before obstruction. This resulted in the restoration of injury in the group reconstituted with CD4^{+} T cells but not in the group reconstituted with CD8^{+} T cells, implying that CD4^{+} T cells are pivotal in the development of injury and fibrosis in this model.

A previous study using severe combined immunodeficient mice did not show any decrease in renal fibrosis compared with WT mice after UUO.[13] This may be partly because of strain difference, as shown in the UUO model.[14] Furthermore, they used a smaller number of mice and examined interstitial volume only, not specifically interstitial fibrosis. A recent study has shown a clear role for CD4^{+} cells in the fibrocyte maturation in UUO,[15] an observation that may provide a mechanism to explain our data.

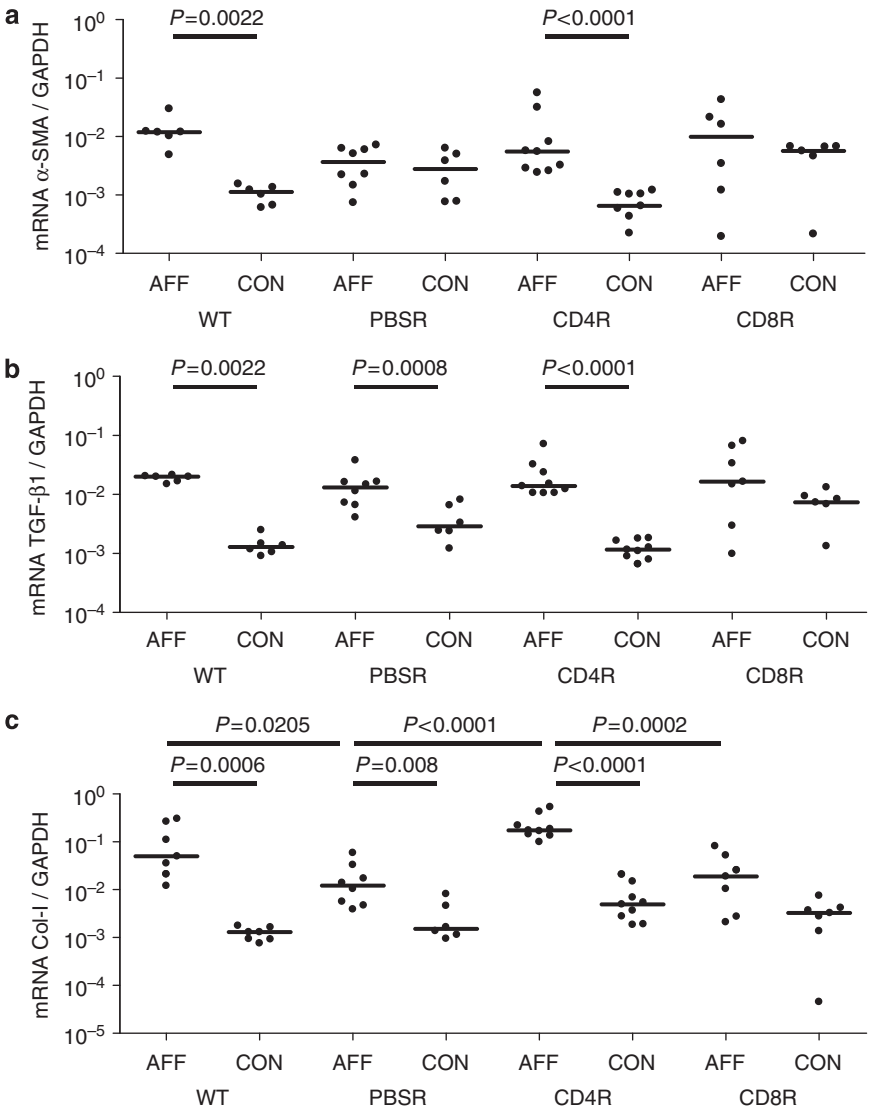

Figure 8 | Quantitative real-time polymerase chain reaction demonstrates UUO-induced upregulation of fibrotic genes in affected kidneys after reconstitution with CD4$^+$ but not with CD8$^+$ T cells. The expression of α-SMA mRNA (**a**), transforming growth factor-β1 mRNA (**b**), and collagen I mRNA (**c**) in affected (AFF) and contralateral (CON) kidneys of WT mice and *RAG*$^{-/-}$ mice injected with saline (PBSR) or reconstituted with CD4$^+$ T cells (CD4R) or CD8$^+$ T cells (CD8R) was measured by quantitative real-time PCR after 14 days of UUO. mRNA expression was normalized to glyceraldehyde 3-phosphate dehydrogenase (GAPDH).

Infiltration of macrophages and T cells has long been known as an early and characteristic feature of renal fibrosis.[1] However, their exact contribution is still unclear.[16,17] Macrophages are thought to be major effector cells in renal fibrosis. For example, blocking CCR2-dependent macrophage infiltration led to a decrease in renal fibrosis in a mouse model.[7] However, activation of macrophages through T-cell cytokines is likely to be crucial in this process. Recently, distinct phenotypes of activated macrophages have been suggested, which enable macrophages to react to different environmental stimuli, some of them T cell dependent.[18] For example, interferon-γ from CD4$^+$ T_H1 cells activates macrophages to an inflammatory phenotype. Alternatively, they can be activated by IL-4 and IL-13, both CD4$^+$ T_H2 cytokines, to facilitate repair processes in surrounding tissue by producing L-proline, a critical substrate for collagen synthesis by fibroblasts.[19] Thus, alternative activation of macrophages could promote fibrotic disease.

However, other studies have shown that the classical activation of macrophages can increase interstitial injury. Alternatively activated macrophages significantly attenuated interstitial injury in adriamycin-induced nephropathy in severe combined immunodeficient mice, whereas classically activated macrophages exacerbated disease, confirming the complex effects of different states of macrophage activation.[20]

When WT, *RAG*$^{-/-}$, or reconstituted *RAG*$^{-/-}$ mice after UUO were compared, we did not observe any difference in the number of macrophages infiltrating the kidney. This does not imply that macrophages do not have a role in UUO-induced renal fibrosis, but suggests that they infiltrate the

kidneys independently of T cells in this model. The presence of different T-cell populations may result in different macrophage activation between groups; however, investigating possibly different macrophage phenotypes was not within the remit of this study.

The number of infiltrating T cells was much higher in reconstituted $RAG^{-/-}$ mice than in WT. This could be due to homeostatic proliferation of the transferred T cells and phenotypic changes effected by this. Along with others, we have shown that T cells rapidly proliferate in a lymphopenic environment, acquiring a memory-like phenotype in the process.[11,21] This memory-like phenotype is likely to enhance their ability to infiltrate the obstructed kidney and could thus lead to the high numbers of T cells observed.

The demonstration of a role for T cells in renal fibrosis supports previous findings implicating lymphocyte function as an important mediator of injury. Immunosuppressive agents such as sirolimus and mycophenolate mofetil have been shown to reduce renal fibrosis in animal models of obstructive nephropathy.[22–25]

Consistent with our results in $RAG^{-/-}$ mice, a study investigating the importance of the leptin signaling pathway in UUO found reduced fibrosis and a reduced number of infiltrating $CD4^+$ T cells in the affected kidneys of leptin-deficient mice, whereas macrophage infiltration was not different from that observed in controls.[26] However, as the reduced numbers of $CD4^+$ T cells occurred in leptin (or leptin receptor)-deficient mice, it was not clear from the study whether the absence of leptin signaling or of $CD4^+$ T cells as such led to the less-severe fibrosis observed in these animals. The reconstitution of $RAG^{-/-}$ mice with $CD4^+$ T cells in this study addresses this question and demonstrates a role for $CD4^+$ T cells in renal fibrosis.

A role for $CD8^+$ T cells in renal fibrosis has been suggested in the context of interstitial fibrosis or tubular atrophy[27] after transplantation.[3] However, our results do not conclusively show an effect of $CD8^+$ T cells on renal fibrosis. This does not exclude an effect of $CD8^+$ T cells, because reconstituted $CD8^+$ T cells may lack cooperation of $CD4^+$ T cells to elicit their effect *in vivo*. Furthermore, the variation in renal fibrosis after reconstitution of $RAG^{-/-}$ mice with $CD8^+$ T cells shows that these cells have the potential to promote renal fibrosis. However, $CD8^+$ T cell-reconstituted animals showed no upregulation of α-SMA, TGF-β1, or collagen I mRNA in affected kidneys compared with contralateral kidneys, whereas all these are upregulated in affected kidneys of WT and $CD4^+$ T cell-reconstituted mice, which might even indicate an antifibrotic role of $CD8^+$ T cells in this model.

The finding of similar levels of TGF-β1 mRNA expression in the affected kidneys of all groups does not necessarily mean a similar activity of TGF-β1 in the affected kidneys, because this primarily depends on cleaving of latent TGF-β1 in the tissue, for example, by matrix metalloproteinase-2 or -9, or cell surface molecules such as αvβ6 integrin. Interestingly, only the upregulation of collagen I mRNA in affected kidneys in animals reconstituted with $CD4^+$ T cells correlated with the histological finding of more severe fibrosis in these animals compared with saline- or $CD8^+$ T cell-reconstituted mice. This suggests that the regulation of collagen I expression by $CD4^+$ T cells is different from that of α-SMA or from the recruitment of α-SMA^+ cells to these kidneys.

Our results show a role for $CD4^+$ T lymphocytes in UUO-induced renal fibrosis. As fibrosis is a common end point for many different types of renal diseases, targeting $CD4^+$ T cells may provide a therapeutic avenue for the prevention of renal injury in patients with progressive renal disease.

METHODS

Animals and surgery

Eight-week-old female C57BL/6 mice (Harlan UK Ltd. (Oxon, UK)) and C57BL/6 $RAG^{-/-}$ mice (kind gift from Professor Gordon Dougan, London[28]) were used in accordance with the Animals (Scientific Procedures) Act 1986. UUO operations were performed as described previously.[29] A volume of 50 μg of anti-CD4 monoclonal antibody (YTA3.1) was administered 1 day before and on the day of UUO, as previously described.[12] Five million $CD4^+$ and $CD8^+$ T cells were purified and used for reconstitution as previously described.[11]

Flow cytometry

Red blood cells were lysed with 1 ml of Lyse Pharm buffer, and labeled with anti-CD4-FITC (clone H129.19, BD Pharmingen, Oxford, UK) and anti-CD8-PerCP (clone 53-6.7, BD Pharmingen) monoclonal antibodies. Samples were acquired using a FACScan cytometer (Beckton Dickinson, Oxford, UK) and analyzed with 'FlowJo' software (Treestar, Ashland, MA, USA).

Tissue harvest

Kidneys were harvested with 4% paraformaldehyde for histological analysis and with optimal cutting temperature compound (Sakura Finetek Europe B.V., The Netherlands) for immunohistochemistry. A section of each kidney was snap frozen for mRNA extraction.

Histology

Periodic acid Schiff's reagent staining was performed on 2 μm sections of paraffin-embedded kidneys. Interstitial expansion was scored on 10 hpf of cortical area per section by superimposing a grid at ×400 magnification and counting the number of points overlying interstitial spaces. Glomerular area was subtracted from the total number of grid intersections. The number of positive intersections was then expressed as a percentage of the whole. The scoring of interstitial collagen deposition as visualized by Martius scarlet blue trichrome staining was performed in the same manner. Line morphometric measurements were used to measure cross-sectional diameters of 10 tubules per hpf, and the tubular area was calculated as ellipse (½ vertical diameter × ½ horizontal diameter × π). The ratio of inner tubular area to outer tubular area, including epithelial cell height, was calculated. All scorings were carried out by observers blinded to the experimental groups.

Immunohistochemistry

Frozen sections (5 μm) were acetone fixed, blocked with 0.3% H_2O_2 in phosphate-buffered saline, followed by Avidin/Biotin block

Table 1 | Primers used for reverse transcriptase-polymerase chain reaction (fw: forward primer, rev: reverse primer)

Name	Sequence	Amplicon size, reference	Position
GAPDH fw	5′-TGG CCT CCA AGG AGT AAG AA-3′	197 bp NM_008084.2 GI: 126012538	1036
GAPDH rev	5′-GTG GGT GCA GCG AAC TTT AT-3′		1232
αSMA fw	5′-CTG ACA GAG GCA CCA CTG AA-3′	160 bp NM_007392.2 GI: 31982518	389
αSMA rev	5′-CAT CTC CAG AGT CCA GCA CA-3′		548
TGF-β1 fw	5′-GTG TGG AGC AAC ATG TGG AA-3′	276 bp NM_011577.1 GI: 6755774	1355
TGF-β1 rev	5′-GGT TCA TGT CAT GGA TGG TG-3′		1630
Col-I fw	5′-TGA CTG GAA GAG CGG AGA GT-3′	202 bp NM_007742.3 GI: 118131144	3867
Col-I rev	5′-GAA TCC ATC GGT CAT GCT CT-3′		4069

Abbreviations: Col, collagen; GAPDH, glyceraldehyde 3-phosphate dehydrogenase; TGF, transforming growth factor.

(Vector Labs, Burlingame, CA, USA) according to the manufacturer's instructions. Tissue sections were stained for CD4 (clone H129.19, BD Pharmingen), CD8 (clone 53-6.7, BD Pharmingen) or F4/80 (clone A3-1, Serotec, Oxford, UK). A biotinylated secondary antibody (BD Pharmingen) was applied and staining was visualized with horse radish peroxidase-conjugated streptavidin (BD Pharmingen) and diaminobenzidine. For α-SMA staining, sections were stained with anti-α-SMA antibody (Sigma–Aldrich, Dorset, UK) and visualized using the EnVision+ System (DAKO UK Ltd., Cambridgeshire, UK) according to the manufacturer's instructions. Immunohistochemical staining for CD4$^+$ or CD8$^+$ cells was analyzed by counting the number of positive cells per hpf at $\times 400$ magnification on 10 fields per section. For analysis of F4/80 and α-SMA staining, a grid was used as described above at a magnification of $\times 1000$ and $\times 250$, respectively. All scorings were carried out by observers blinded to the experimental groups.

Reverse transcription quantitative real-time PCR

RNA was extracted using the Trizol method (Invitrogen, Paisley, UK) according to the manufacturer's instructions. A volume of 1 μg of RNA was reverse transcribed using SuperScript II reverse transcriptase and Oligo(dT) primers (Invitrogen). The mRNA expression of α-SMA, TGF-β1, and collagen I was quantified using SYBR Green master mix (Finnzyme, New England Biolabs, UK) and glyceraldehyde 3-phosphate dehydrogenase for normalization among samples. Primers were designed using Primer3 software (The Whitehead Institute, Cambridge, MA, USA)[30] and tested on 'noRT' controls to ensure that they do not amplify genomic DNA. PCRs were performed as 40 cycles of 95 °C (15 s), 60 °C (45 s), and 72 °C (45 s) on a Chromo4 cycler and recorded with MJ Opticon Monitor software V3 (Biorad Labs Inc., Hercules, CA, USA). Gene expression was calculated relative to glyceraldehyde 3-phosphate dehydrogenase expression as described before.[31] The primers used are listed in Table 1.

Statistical analysis

The unpaired Mann–Whitney *U*-Test was used to compare groups with each other after the Kruskal–Wallis test had shown significant differences ($P<0.05$) between different UUO groups. Data were analyzed using Prism4 software (Graph Pad Software, San Diego, CA, USA) and are given as mean ± s.e.

DISCLOSURE

All the authors declare no competing interests.

ACKNOWLEDGMENTS

TTT was funded by the Sarah Agboola PhD Studentship of the Guy's and St Thomas' Kidney Patients' Association.

SUPPLEMENTARY MATERIAL

Figure S1. Accumulation of α-SMA$^+$ cells is not impaired by antibody-mediated depletion of CD4$^+$ cells.
Supplementary material is linked to the online version of the paper at http://www.nature.com/ki

REFERENCES

1. Harris RC, Neilson EG. Toward a unified theory of renal progression. *Annu Rev Med* 2006; **57**: 365–380.
2. Bohle A, Strutz F, Muller GA. On the pathogenesis of chronic renal failure in primary glomerulopathies: a view from the interstitium. *Exp Nephrol* 1994; **2**: 205–210.
3. Robertson H, Ali S, McDonnell BJ *et al.* Chronic renal allograft dysfunction: the role of T cell-mediated tubular epithelial to mesenchymal cell transition. *J Am Soc Nephrol* 2004; **15**: 390–397.
4. Anders HJ, Vielhauer V, Frink M *et al.* A chemokine receptor CCR-1 antagonist reduces renal fibrosis after unilateral ureter ligation. *J Clin Invest* 2002; **109**: 251–259.
5. Vielhauer V, Anders HJ, Mack M *et al.* Obstructive nephropathy in the mouse: progressive fibrosis correlates with tubulointerstitial chemokine expression and accumulation of CC chemokine receptor 2- and 5-positive leukocytes. *J Am Soc Nephrol* 2001; **12**: 1173–1187.
6. Eis V, Luckow B, Vielhauer V *et al.* Chemokine receptor CCR1 but not CCR5 mediates leukocyte recruitment and subsequent renal fibrosis after unilateral ureteral obstruction. *J Am Soc Nephrol* 2004; **15**: 337–347.
7. Kitagawa K, Wada T, Furuichi K *et al.* Blockade of CCR2 ameliorates progressive fibrosis in kidney. *Am J Pathol* 2004; **165**: 237–246.
8. Zheng G, Wang Y, Mahajan D *et al.* The role of tubulointerstitial inflammation. *Kidney Int Suppl* 2005; **94**: S96–S100.
9. Tipping PG, Holdsworth SR. T cells in crescentic glomerulonephritis. *J Am Soc Nephrol* 2006; **17**: 1253–1263.
10. Mombaerts P, Iacomini J, Johnson RS *et al.* RAG-1-deficient mice have no mature B and T lymphocytes. *Cell* 1992; **68**: 869–877.
11. Moxham VF, Karegli J, Phillips RE *et al.* Homeostatic proliferation of lymphocytes results in augmented memory-like function and accelerated allograft rejection. *J Immunol* 2008; **180**: 3910–3918.
12. Wong W, Morris PJ, Wood KJ. Syngeneic bone marrow expressing a single donor class I MHC molecule permits acceptance of a fully allogeneic cardiac allograft. *Transplantation* 1996; **62**: 1462–1468.
13. Shappell SB, Gurpinar T, Lechago J *et al.* Chronic obstructive uropathy in severe combined immunodeficient (SCID) mice: lymphocyte infiltration

is not required for progressive tubulointerstitial injury. *J Am Soc Nephrol* 1998; **9**: 1008–1017.
14. Puri TS, Shakaib MI, Chang A *et al.* Chronic kidney disease induced in mice by reversible unilateral ureteral obstruction is dependent on genetic background. *Am J Physiol Renal Physiol* 2010; **298**: F1024–F1032.
15. Niedermeier M, Reich B, Rodriguez Gomez M *et al.* CD4+ T cells control the differentiation of Gr1+ monocytes into fibrocytes. *Proc Natl Acad Sci USA* 2009; **106**: 17892–17897.
16. Nikolic-Paterson DJ, Lan HY, Hill PA *et al.* Macrophages in renal injury. *Kidney Int Suppl* 1994; **45**: S79–S82.
17. Strutz F, Neilson EG. The role of lymphocytes in the progression of interstitial disease. *Kidney Int Suppl* 1994; **45**: S106–S110.
18. Gordon S. Alternative activation of macrophages. *Nat Rev Immunol* 2003; **3**: 23–35.
19. Wynn TA. Fibrotic disease and the T(H)1/T(H)2 paradigm. *Nat Rev Immunol* 2004; **4**: 583–594.
20. Wang Y, Wang YP, Zheng G *et al. Ex vivo* programmed macrophages ameliorate experimental chronic inflammatory renal disease. *Kidney Int* 2007; **72**: 290–299.
21. Murali-Krishna K, Ahmed R. Cutting edge: naive T cells masquerading as memory cells. *J Immunol* 2000; **165**: 1733–1737.
22. Wu MJ, Wen MC, Chiu YT *et al.* Rapamycin attenuates unilateral ureteral obstruction-induced renal fibrosis. *Kidney Int* 2006; **69**: 2029–2036.
23. Badid C, Vincent M, McGregor B *et al.* Mycophenolate mofetil reduces myofibroblast infiltration and collagen III deposition in rat remnant kidney. *Kidney Int* 2000; **58**: 51–61.
24. Bayazit AK, Bayazit Y, Noyan A *et al.* Comparison of mycophenolate mofetil and azathioprine in obstructive nephropathy. *Pediatr Nephrol* 2003; **18**: 100–104.
25. Goncalves RG, Biato MA, Colosimo RD *et al.* Effects of mycophenolate mofetil and lisinopril on collagen deposition in unilateral ureteral obstruction in rats. *Am J Nephrol* 2004; **24**: 527–536.
26. Kumpers P, Gueler F, Rong S *et al.* Leptin is a coactivator of TGF-beta in unilateral ureteral obstructive kidney disease. *Am J Physiol Renal Physiol* 2007; **293**: F1355–F1362.
27. Solez K, Colvin RB, Racusen LC *et al.* Banff '05 Meeting Report: differential diagnosis of chronic allograft injury and elimination of chronic allograft nephropathy ('CAN'). *Am J Transplant* 2007; **7**: 518–526.
28. Simmons CP, Clare S, Ghaem-Maghami M *et al.* Central role for B lymphocytes and CD4+ T cells in immunity to infection by the attaching and effacing pathogen Citrobacter rodentium. *Infect Immun* 2003; **71**: 5077–5086.
29. Tapmeier TT, Brown KL, Tang Z *et al.* Reimplantation of the ureter after unilateral ureteral obstruction provides a model that allows functional evaluation. *Kidney Int* 2008; **73**: 885–889.
30. Rozen S, Skaletsky HJ. Primer3. In, The Whitehead Institute of Biomedical Research, 1998.
31. Pfaffl MW. A new mathematical model for relative quantification in real-time RT-PCR. *Nucleic Acids Res* 2001; **29**: e45.